EXPERIMENTAL STUDY ON NAVIGATION FOR WHEAT SEEDLING ROOT CUTTING BASED ON DEEP LEARNING
/
基于深度学习的麦苗断根导航实验研究

HaiBo LIN [*1,2], Chenhe XU [1,2], Yuandong LU [3] [1]
[1] School of Mechanical & Automotive Engineering, Qingdao University of Technology, Qingdao 266520, China
[2] Key Lab of Industrial Fluid Energy Conservation and Pollution Control (Qingdao University of Technology), Ministry of Education, Qingdao 266520, China
[3] Shandong Lingong Construction Machinery Co., Ltd., Shandong 016000, China
Email: linhaibo@qut.edu.cn; 871306176@qq.com; 1214398056@qq.com
DOI: https://doi.org/10.35633/inmateh-71-45

Keywords: *Deep learning, Agricultural machinery navigation line, Field experiment, Complex conditions, Algorithm robustness.*

ABSTRACT
In response to the automatic extraction of navigation lines for wheat root cutting, this paper conducted field experiments and analyses on the navigation line extraction algorithm, based on the improved YOLOv5 algorithm. Firstly, based on the characteristics of wheat seedling rows during the wheat rejuvenation period, the YOLOv5 algorithm was improved by using rotation detection box labels, and navigation lines were extracted by fitting the detection boxes using clustering methods. Then, an experimental system was established to conduct field experiments on the algorithm: (1) Tests were conducted at three speeds of 0.5 m/s, 1.0 m/s and 1.5 m/s respectively, and the position error of the root cutter was measured and analyzed, indicating that the actual navigation path position error increased with the speed. The best navigation performance was observed at 1 m/s, with an average positional error of 18.56 mm, meeting the requirements for wheat root cutting. (2) Robustness analysis of the algorithm was conducted using data collected from 2019 to 2022. Comparative tests were conducted from four aspects: different years, different time periods, different environments, and different yaw angles. The results showed that the algorithm proposed in this paper has stronger robustness and higher accuracy.

摘要
针对小麦断根导航线自动提取的问题，本文在改进 YOLOv5 算法的基础上，对导航线提取算法进行了田间实验测试和分析。首先，针对小麦返青期麦苗行的特点，用旋转检测框标识对 YOLOv5 算法进行改进，通过聚类方法对检测框拟合进行导航线的提取；然后，搭建实验系统对算法进行田间实验：（1）分别在 0.5m/s、1.0m/s、1.5m/s 三个速度下进行测试，测量分析断根刀的位置误差，表明实际导航路径位置误差随行进速度的增加而变大，1m/s 时导航效果最好，位置误差平均值为 18.56mm，满足小麦断根要求；（2）利用 2019-2022 年采集数据对对算法的鲁棒性进行实验分析，从不同年份、不同时段、不同环境及不同偏航角四个方面进行对比测试，结果表明本文算法鲁棒性更强、准确性更高，能够满足作业实时性要求。

INTRODUCTION
As one of the main food crops in China, the increase in wheat production is of great significance for the security of food in our country *(Jiang et al., 2021)*. As early as the 1960s and 1970s, *Yu et al (1985)* from Shandong Agricultural University studied the methods of increasing the yield of winter wheat and found that deep tillage and root-cutting operation during the rejuvenation period of winter wheat could promote the development of wheat roots and increase the yield significantly. Later, *Lv et al, (2006),* developed a set of small wheat root-cutting machine, which showed that mechanical root-cutting measures could increase the yield by 9.96%-11.4%. However, the machine needs to continuously adjust its posture during the operation process, ensuring that the wheels do not press against the wheat seedlings, while also preventing the root cutter from damaging the wheat seedlings, which is time-consuming and laborious for manual operation, and has low production efficiency. Therefore, it is necessary to develop a root cutting machine that can automatically navigate the wheat seeding line.

[1] *Lin Haibo, PhD, Lecturer; Xu Chenhe, MS; Lu Yuandong, MS*

At present, agricultural machinery in precision agriculture mainly uses satellite navigation systems such as Beidou and GPS for navigation and positioning *(Dhruba et al., 2018)*. However, the use of satellite navigation will face problems such as high equipment prices and unstable systems *(Sevilla et al., 2021)*. Moreover, the accuracy of satellite navigation is suitable for field operations, but it is not suitable for precision navigation of roots cutting. In recent years, machine vision and image processing technology has developed rapidly, and it has begun to be applied in various aspects such as field agricultural machinery navigation, variable spraying and weed identification (*He et al., 2021; Yun et al., 2021; Jeon et al., 2021; Li et al., 2021*). However, the application of this technology in the early wheat field navigation is less and not suitable, mainly because the wheat field environment is complex and diverse: (1) variations in lighting due to time differences and weather changes; (2) the shape of wheat seedlings in different growth periods was different; (3) the wheat field was affected by weeds, leaves and other debris; (4) shadows caused by agricultural machinery, power poles, and trees; (5) in the process of agricultural machinery operation, there is a certain yaw angle in the camera during the image acquisition process due to uneven ground or mechanical vibration. Therefore, how to provide a visual navigation line with strong robustness and high accuracy in a complex environment has become the hot sport of current research.

In recent years, deep learning has begun to be applied to the agricultural field, which has a wide range of applications in crop detection, but there are few reports on wheat field navigation applications. In this paper, a method of wheat seedling navigation line extraction based on deep learning was proposed, and field experiments were carried out to verify the reliability of the algorithm through field tests *(Liu et al., 2020; Pang et al., 2020; Khan et al., 2021; Liu et al., 2020; Villacrés et al., 2023; Amrani et al., 2023; Yadav et al., 2023)*.

MATERIALS AND METHODS

In response to the complexity of wheat field environments *(Jiang et al., 2016)*, this paper adopts the YOLOv5 algorithm model in deep learning to detect wheat seedlings and avoid the interference of weeds and other environmental background factors. Object detection algorithms have found widespread use in crop detection. However, there are not many studies on it used to detect crop rows, mainly because the algorithm usually uses a horizontal detection box to identify the target, and the crop rows in the image have a certain length and tilt angle. If the crop rows are marked in the whole column, it will inevitably lead to more soil background areas in the box and include other row crops, which is not conducive to the training of the model. In this regard, this paper uses a rotatable detection box to identify the position of wheat rows. It adds angle parameters to the horizontal detection frame, which is responsible for detecting the rotation of the frame.

Algorithm Improvement

Because the detection boxes with larger length and width are more sensitive to the angle change, the current main angle regression prediction method has the problem of boundary discontinuity. This will cause the loss value of the model to surge at the boundary, resulting in the detection accuracy of the algorithm is low at the boundaries *(Yang et al., 2019)*. In this paper, the angle prediction for object detection boxes is treated as a classification problem. To enhance the tolerance for errors between adjacent angles, a circular smooth label (CSL) *(Yang and Yan, 2020)* is introduced, tailored to the wheat field scene. This approach aims to improve the robustness of angle prediction within detection boxes.

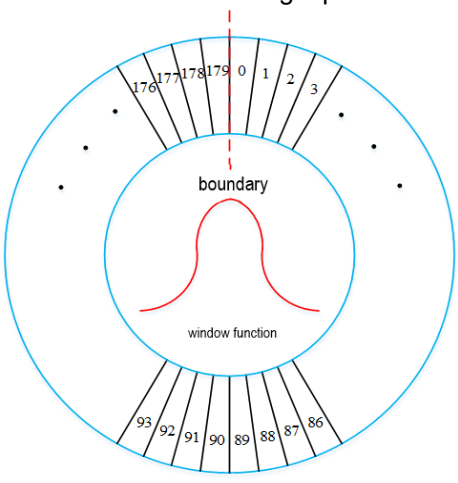

Fig. 1 - CSL schematic

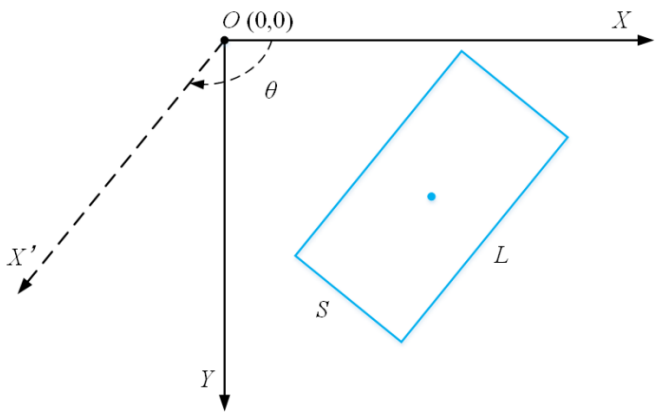

Fig. 2 - The schematic of rotation angle definition

The CSL schematic is shown in Figure 1, and the CSL is calculated as follows:

$$CSL(x)=\begin{cases} g(x) & \theta-r<x<\theta+r \\ 0 & \text{otherwise} \end{cases} \tag{1}$$

$$g(x)=ae^{-\frac{(x-b)^2}{2c^2}} \tag{2}$$

where, $g(x)$ represents the window function, here is the Gaussian function; r is the radius of the window function, which is taken here as 6; θ is the rotation angle of the detection box; a, b, and c are constants.

The angle range of CSL here is [0º, 180º). In Figure 1, 0º coincides with 180º, so only one of them is chosen. The parameters of the rotating detection box are expressed as (r_x, r_y, L, S, θ), where r_x and r_y are the horizontal and vertical coordinates of the center point of the box respectively, L is the long side of the box, and S is the short side of the box, the definition of the rotation angle θ is shown in Figure 2, which is the angle rotated by clockwise rotation along the X-axis direction to parallel with the long side of the detection box. To assess the effectiveness of angle prediction, a binary cross-entropy loss function, BCE With LogitsLoss, is employed to compute the angle loss. The formula for calculating the loss is as follows:

$$\begin{cases} loss(z,y)=\text{mean}\left\{l_0,\cdots,l_{N-1}\right\} \\ l_n=\text{sum}\left\{l_{n,0},l_{n,1},\cdots,l_{n,179}\right\} \\ l_{n,i}=-\left[y_{n,i}\ln\left(\delta\left(z_{n,i}\right)\right)+\left(1-y_{n,i}\right)\ln\left(1-\delta\left(z_{n,i}\right)\right)\right] \\ y_{n,i}=CSL(x) \end{cases} \tag{3}$$

where: N represents the number of samples; $i\in[0,180)$, divided into 180 categories; δ is the sigmoid function; $Z_{n.i}$ represents the probability of the i^{th} angle when predicting the n^{th} sample, when the value is 1, that is, the predicted value; $y_{n,i}$ represents the label value (true value) of the i^{th} angle calculated in $CSL(x)$ for the n^{th} sample. By substituting the predicted value of each rotation angle of the N^{th} sample and the true value into $l_{n,i}$, the 180 angle results of the N^{th} sample are obtained by summation, find the average of the calculated results of N samples, that is the loss value of the predicted angle. After adding the angle prediction branch, the number of channels in the output feature map becomes (1+4+a+180)×3.

Navigation line extraction

The R-YOLOv5 algorithm model in this paper identifies the whole row of wheat seedlings, that is, one row of wheat seedlings outputs one detection box. But in the actual output result, there may be multiple detection boxes corresponding to one row of wheat seedlings, so it is necessary to cluster detection boxes belonging to the same wheat seedlings. This paper proposes an adaptive clustering method for detection boxes of peer wheat seedlings. The specific steps are as follows:

Step 1: Define a data set $Data=\left\{Box_1\left(r_x^1,r_y^1,L^1,S^1,\theta^1\right),\cdots,Box_n\left(r_x^n,r_y^n,L^n,S^n,\theta^n\right)\right\}$ to store the parameters of the output detection box, where $r_x^i,r_y^i,L^i,S^i,\theta^i$ respectively represent the horizontal coordinate of the center point, the vertical coordinate of the center point, the long side, the short side and the rotation angle, n represents the number of detection boxes of an image output;

Step 2: Randomly select a detection box from the data set *Data* Box_i, add it to the data set, and $Class_1$ delete it from the data set;

Step 3: According to the parameters of the detection box Box_i to find out the center point of the box and parallel to the long side of the line equation $l_i: y=-\tan\theta^i x+r_y^i+\tan\theta^i r_x^i$, and then randomly select the detection box Box_j from the data set Data, calculate the distance between the center point of the box and the line l_i $d_{ij}=\left|\frac{\tan\theta^i\left(r_x^j-r_x^i\right)+r_y^j-r_y^i}{\sqrt{1+\left(\tan\theta^i\right)^2}}\right|$. If $d_{ij}<\frac{S^j}{2}$, then the detection box Box_j is deleted from the data set Data, and the data set is added into $Class_1$,otherwise, no operation is performed;

Step 4: Repeat step 3 to complete all the boxes in the data set Data, and finally get the data set that belongs to the wheat seedling detection box in the same row $Class_1$;

Step 5: Repeat step 2-3, finally get the data set $Class_1$,..., $Class_m$, m represents the number of rows of wheat seedlings.

The adaptive clustering results of the wheat seedling detection frame are shown in Figure 3. Figure 3(1) is the detection frame output by the R-YOLOv5 algorithm model before clustering. At this time, each detection frame is relatively independent. Figure 3(2) shows that after the adaptive clustering method is adopted, the detection boxes belonging to the same row of wheat seedlings are divided into one class, and the detection boxes belonging to the same row of wheat seedlings are set to the same color. The center line of the detection box in the same cluster is the row line of wheat seedlings.

(1) detection boxes before clustering (2) detection boxes after clustering

Fig. 3 - The adaptive clustering result of detection box

Experimental Platform

In this paper, field experiments are conducted to verify the navigation line fitting performance of the algorithm.

The experiment in this paper is based on the experimental platform of automatic row control system for wheat root-cutting fertilization developed by the author's project team, as shown in Figure 4. The mechanical device mainly consists of two parts: traction device and wheat root-cutting fertilization device.

Fig. 4 - Experimental platform mechanical device

The traction device of the experimental platform is an 80hp KAI WO 804 tractor, and the wheat root-cutting fertilization device is connected by a three-point suspension device. The wheat root-cutting fertilization device is shown in Figure 5. The device is equipped with multiple root-cutter, and their distance is 30 cm according to the planting spacing design.

Each root cutter is welded with a small round tube at the back and connected with a white plastic tube for spreading fertilizer and preventing fertilizer from splashing outside; the camera is installed on the upper end of the second root cutter, which is circled blue in the figure, the camera is about 50 cm from the ground, the pitch angle is set to 45°, the yaw angle is set to 0°, and the pixel is 1920×1080; the root cutters can move left and right driven by the motor device.

Fig. 5 - Partial structure of wheat root cutting fertilization device

The control system is composed of industrial computer, control board, motor and motor driver. After the wheat seedling images are collected by the camera, the industrial computer extracts the wheat seedling navigation line, then, calculates the deviation, and sends the deviation information to the control board. The control board outputs the corresponding control signal to the motor to drive the motor to navigate the line.

Experimental Process

The field experiment of this paper was conducted at the "Intelligent Root Cutting and Layered Fertilization Technology and Equipment Experimental Demonstration Base for Wheat" in Jiaonan, Qingdao, Shandong Province. In the process of the experiment, the manual driving tractor provided the power, and the automatic alignment of the wheat root-cutting fertilization device pulled behind was completed by the control system based on the algorithm in this paper, as shown in Figure 6. In addition, due to the complex environment of the wheat field, it is difficult to subdivide various single cases, so the navigation performance of the proposed algorithm is verified by controlling different forward speeds of the experimental platform instead of conducting specific test analysis in a single case. In order to simplify the test and facilitate the measurement, fertilization is not carried out during the traveling process.

Fig. 6 - The field test

As for the measurement of the position error of the actual navigation path, the position error was measured by two people every 0.5 m, and the average value was taken. The experimental platform is installed with 4 root cutters. Since the distances between root cutters and wheat planting are both 30 cm, the position error of the traveling path of one root cutter is only needed to be measured. The path corresponding to the root cutter equipped with a camera is selected for measurement in this test.

The position error measurement method of the actual path is shown in Figure 7, where A represents the soil area before the root cutting, B represents the wheat seedling area, C represents the soil area after the root cutting, l_1, l_2 respectively represents the accurate wheat seedling line, and l_3, l_4 respectively represents the line at the top of the protruding sides of the ditch cut by the root cutter. The specific measurement steps are as follows:

Step 1: Measure the distance between l_1, l_2 each position, and find the midpoint o_1 of the distance between the two rows of wheat seedlings, which is the accurate position;

Step 2: Measure the distance between l_3, l_4 the corresponding position, find the middle point o_2 of the top of the protrusion on both sides of the ditch, the point is the actual position of the cutter;

Step 3: Measuring the distance between o_1, o_2 the two points in the vertical wheat seedling line direction, that is, the position error of the root cutter traveling at the position point;

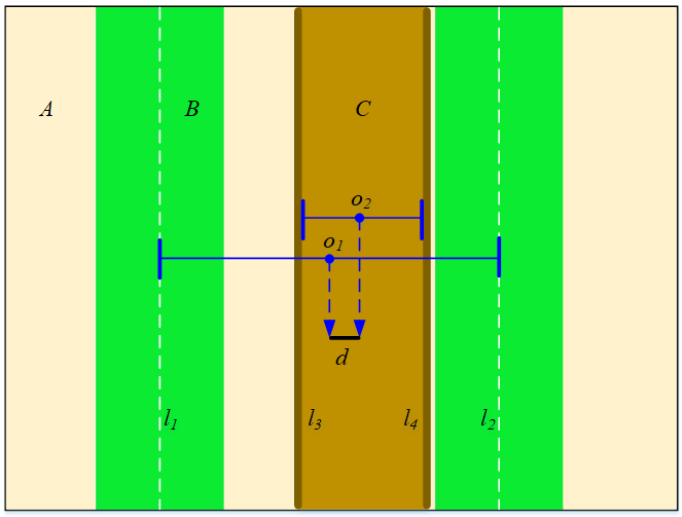

Fig. 7 - The schematic of position error measurement method

According to the papers of *Huo et al., (2004); Li and Zhu, (2006)*, the traveling speed of wheat root-cutting machine is usually 1.7 5 km/h (about 0.47-1.39 m/s), so the experiment set the forward speed of the platform in this paper as 0.5 m/s, 1.0 m/s and 1.5 m/s respectively. In each group of experiments, the distance of the platform at the set speed is about 30 m. Since the speed of the platform at the starting point and the end is unstable, select the middle section with a stable speed and a length of 20 m to measure the position error of the path of the root cutter. According to the position error measurement method, the error of 20 position points is measured in each group, as shown in Figure 8.

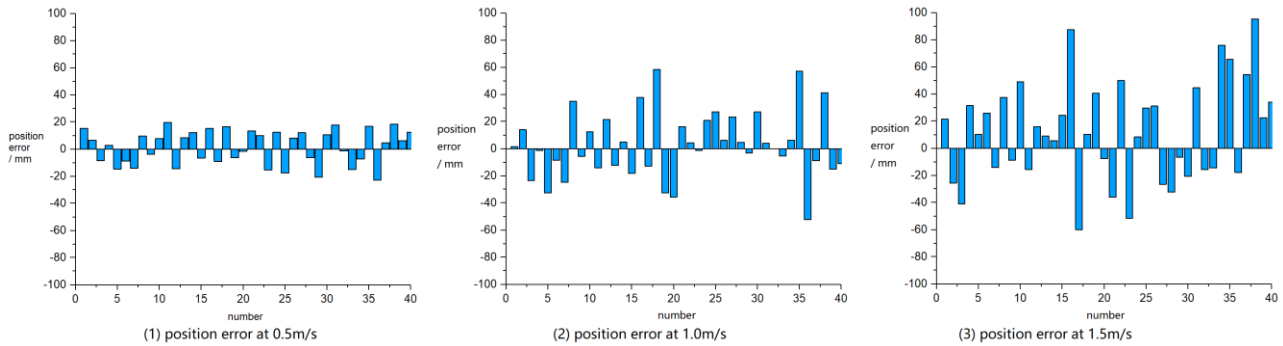

Fig. 8 - Position errors at different speeds

The maximum, average, and standard deviation of the navigation path position error at 0.5 m/s, 1.0 m/s, and 1.5 m/s were calculated. Based on the measurement results, when the traveling speed of the experimental platform is 0.5 m/s, the maximum, average and standard deviation of the position error are 22 mm, 11.27 mm and 2.32 mm, respectively. When the traveling speed of the experimental platform is 1.0 m/s, the maximum, average and standard deviation of the position error are 58 mm, 18.56 mm and 3.96 mm, respectively. When the traveling speed of the experimental platform is 1.5 m/s, the maximum, average and standard deviation of the position error are 95 mm, 31.9 mm and 4.72 mm, respectively.

The measurement results of the root cutters of the platform at different speeds show that the average and standard deviation of the actual navigation path position error increase with the speed during the platform moving. This phenomenon indicates that the faster speed, the more unstable the navigation effect. When the platform travels at a fast speed, it is subject to the calculation time of the upper computer and the response time of the lower computer of the control system. The positions of the root cutters cannot be corrected in time, resulting in a large position deviation.

Usually, the distance between the accurate path and the root of the wheat seedling on both sides is about 10 cm, and the maximum position error of the algorithm in the experiment is 95 mm. By observing the path of the root cutter, it is found that the wheat seedling is not accidentally injured. Therefore, the visual navigation provided by the algorithm for the automatic row control system of wheat root cutting meets the requirement that the root cutter does not hurt the seedling. Based on the experiment in this paper, it is also found that the navigation effect is best when the system operates at 1 m/s. When the navigation speed is lower than this speed, although the navigation accuracy is high, the operation efficiency is relatively low; when above this speed, the navigation accuracy decreases.

RESULTS

In order to verify the robustness and real-time navigation of the proposed algorithm, relevant images were selected from the accumulated data from 2019-2022, comparing the effects of the proposed algorithm and the improved algorithm from four aspects: different years, different periods of rejuvenation, different environments and different yaw angles. It was analyzed by combining distance error and angle error.

Comparative analysis of robustness of the algorithm

Since the wheat seedling lines involved in navigation line extraction usually pass through the upper and lower edges of the image, the algorithm proposed previously only targets at the wheat seedling lines that pass through the upper and lower edges of the image at the same time. Here, only the distance error and angle error of the wheat seedling line are counted, which are the same as the above conditions.

Comparison of wheat seedling line extraction in different years

In the wheat fields of different years, the soil moisture content will be different, and the growth state of wheat seedlings will be different, so the influence of wheat seedling images of different years on the two algorithms is analyzed here.

As shown in Figure 9, the images were respectively collected in March 2019-2022. It can be seen from the figure that the color of wheat seedlings and soil background in different years are quite different. Among which the soil moisture content in 2019 is relatively small, and the wheat seedlings have more dead leaves. Judging from the effect of wheat seedling line extraction, the two algorithms can obtain relatively accurate wheat seedling line. The algorithm in this paper can also extract the wheat seedling line on both sides of the image, but its accuracy is not as high as that in the middle of the image.

Fifty images were randomly selected for testing in each year, and the distance error and angle error were counted, as shown in Table 1. It can be seen from the table that each algorithm has little difference in various statistical indicators of the four years, indicating that the two algorithms have certain adaptability to wheat seedling images of different years. In addition, by comparing the two algorithms, it can be found that the distance error and angle error of the proposed algorithm are both smaller than that of the previous algorithm, which indicates that the proposed algorithm is more robust than the previous algorithm.

Table 1

The evaluation statistics of wheat seedling lines in different years under two algorithms

Algorithm	Categories	Range error / pixel	Angle error / °
Textual algorithm	In 2019	10.61	0.86
	In 2020	8.26	0.61
	In 2021	9.80	0.67
	In 2022	11.15	0.83
	Average	9.95	0.74
Previous algorithm	In 2019	19.55	1.64
	In 2020	15.37	1.43
	In 2021	23.62	1.79
	In 2022	15.86	1.56
	Average	18.60	1.60

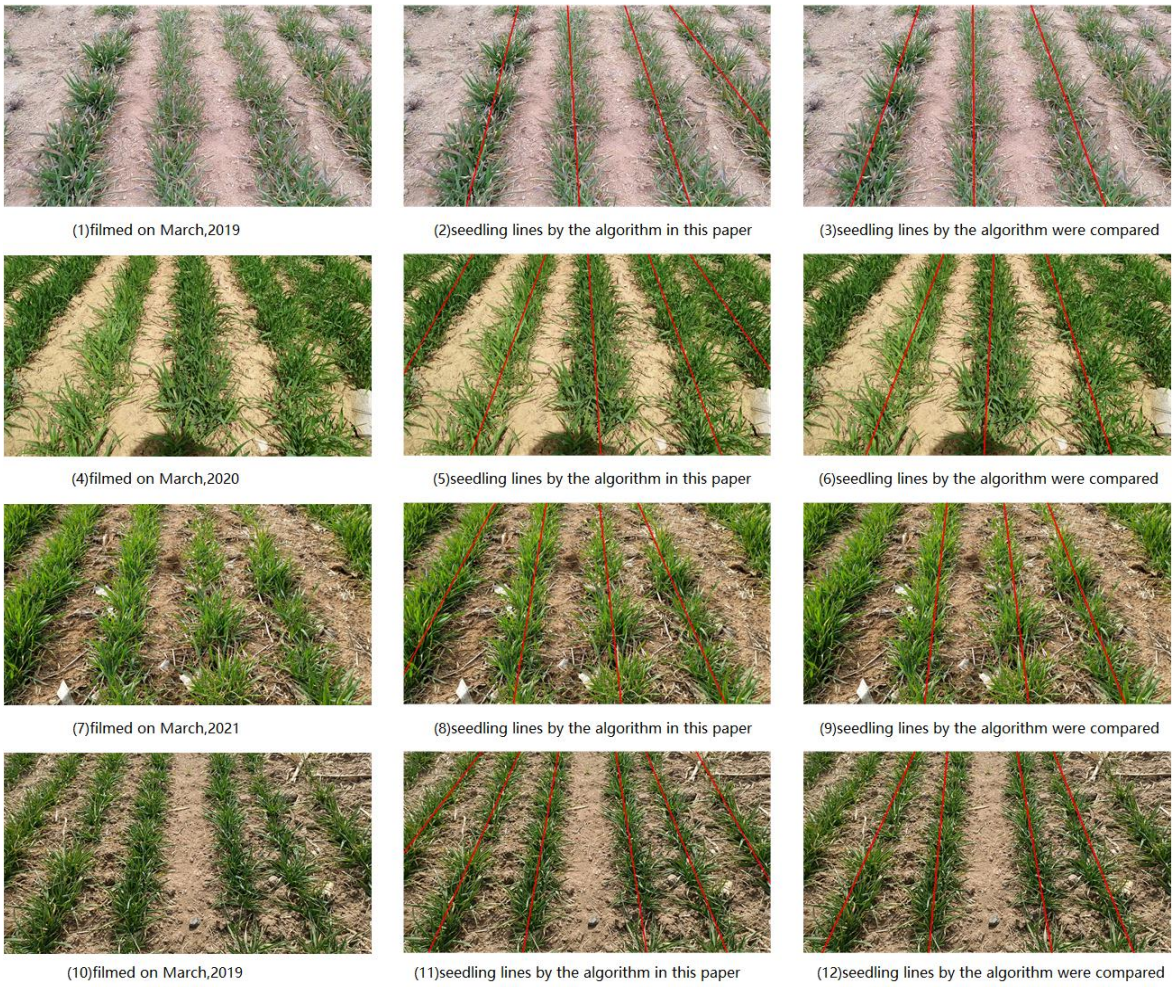

Fig. 9 - The wheat seedling lines in different years obtained by two algorithms

Wheat seedling line extraction and comparison in different periods of rejuvenation stage

The wheat that entered the rejuvenation stage began to grow and develop.

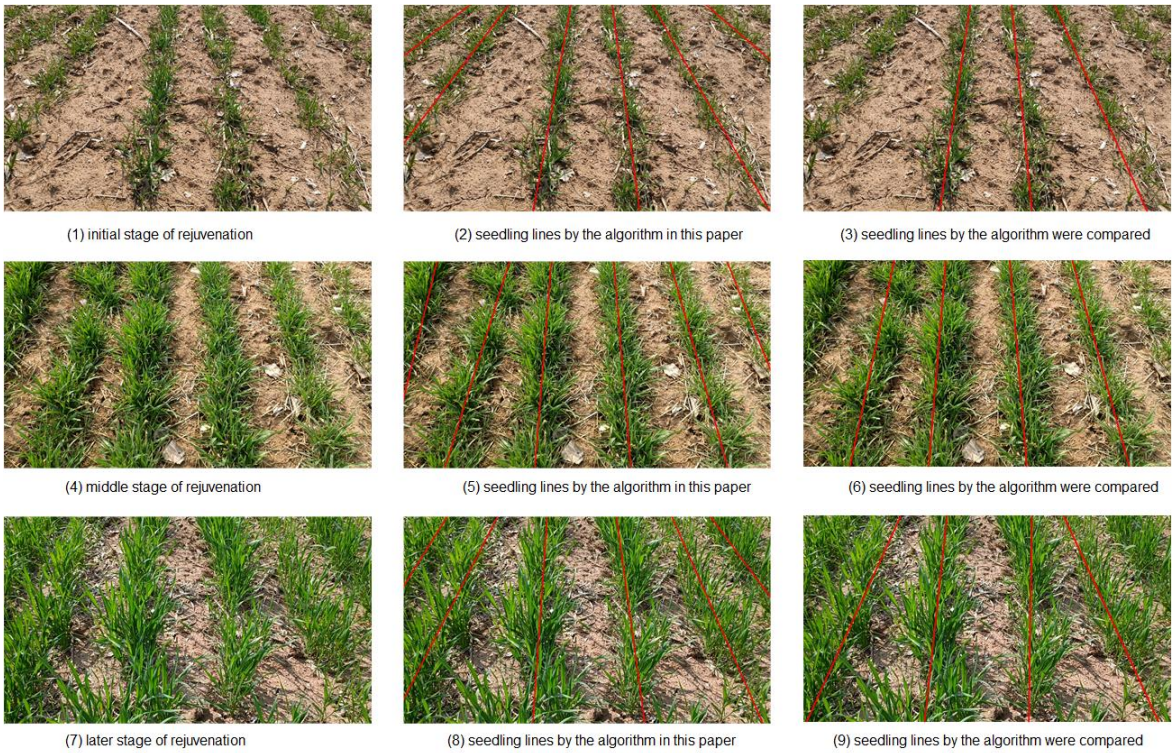

Fig. 10 - The wheat seedling lines at different time in rejuvenation period obtained by two algorithms

In Figure 10(1), the wheat seedlings in the early rejuvenation stage were collected at the end of February, when the wheat seedlings were sparse; in Figure 10(2), the wheat seedlings in the middle of the rejuvenation stage were collected in mid-March, when the wheat seedlings were flourishing; in Figure 10(3), the wheat seedlings at the later stage of rejuvenation were collected at the beginning of April, at which time the wheat seedlings began to joint, which showed a big difference in their appearance morphology. Therefore, the influence of wheat seedlings in different time periods of the rejuvenation period on the two algorithms is analyzed here. In the figure, the wheat seedlings in each time period obtained by the algorithm in this paper are more accurate, while the wheat seedlings in the late rejuvenation period obtained by the previous algorithm are slightly less accurate.

Table 2

The evaluation statistics of wheat seedling lines at different time under two algorithms

Algorithm	Categories	Range error / pixel	Angle error / °
Textual algorithm	Initial stage	10.52	1.06
	Middle stage	9.36	0.89
	Later stage	13.61	1.15
	Average	11.16	1.03
Previous algorithm	Initial stage	22.67	1.79
	Middle stage	16.34	1.53
	Later stage	31.64	3.06
	Average	18.5	2.12

Table 2 shows the evaluation statistics of 50 wheat seedling images at different time periods in the rejuvenation stage. As can be seen from the table, the extraction accuracy of the proposed algorithm is significantly better than that of the previous algorithm, especially in the late period of rejuvenation.

The distance error and angle error of the previous algorithm are twice as much as that of the proposed algorithm. In addition, the phenomenon of wheat seedling line leakage exists in the previous algorithm, which indicates that the robustness of the previous algorithm is not strong enough. The table also indicates that both methods exhibit relatively smaller errors in wheat seedling images from the mid-rejuvenation phase, indicating that the navigation lines extracted during this period are more accurate and suitable for wheat root-cutting by automatic row method.

Comparison of wheat seedling line extraction under different environmental backgrounds

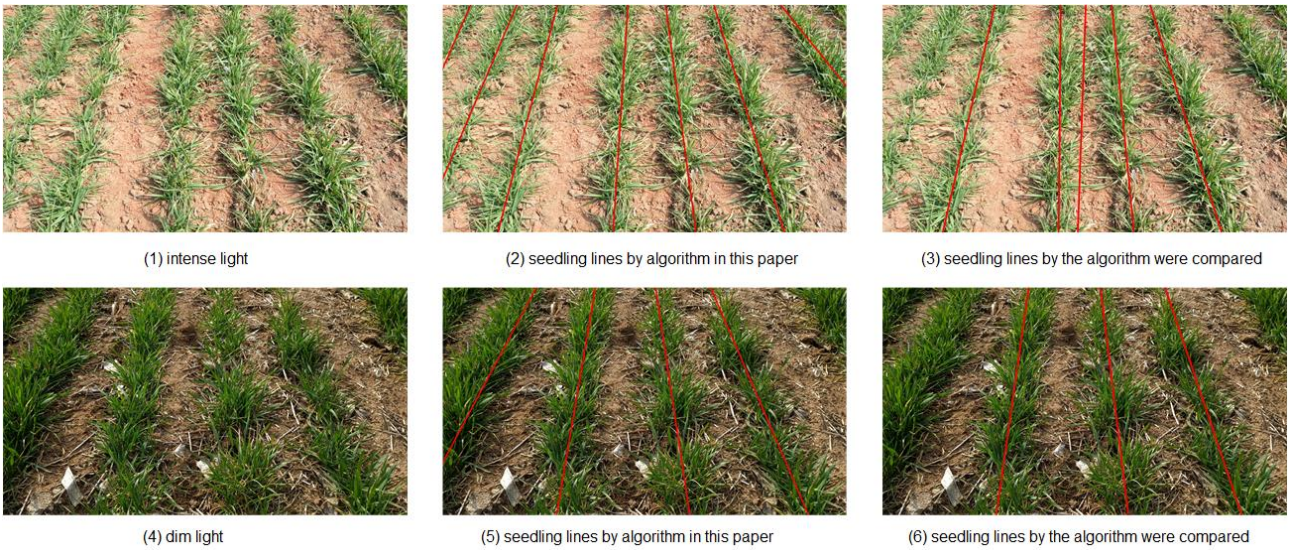

Fig. 11 - The wheat seedling lines under different illumination obtained by two algorithms

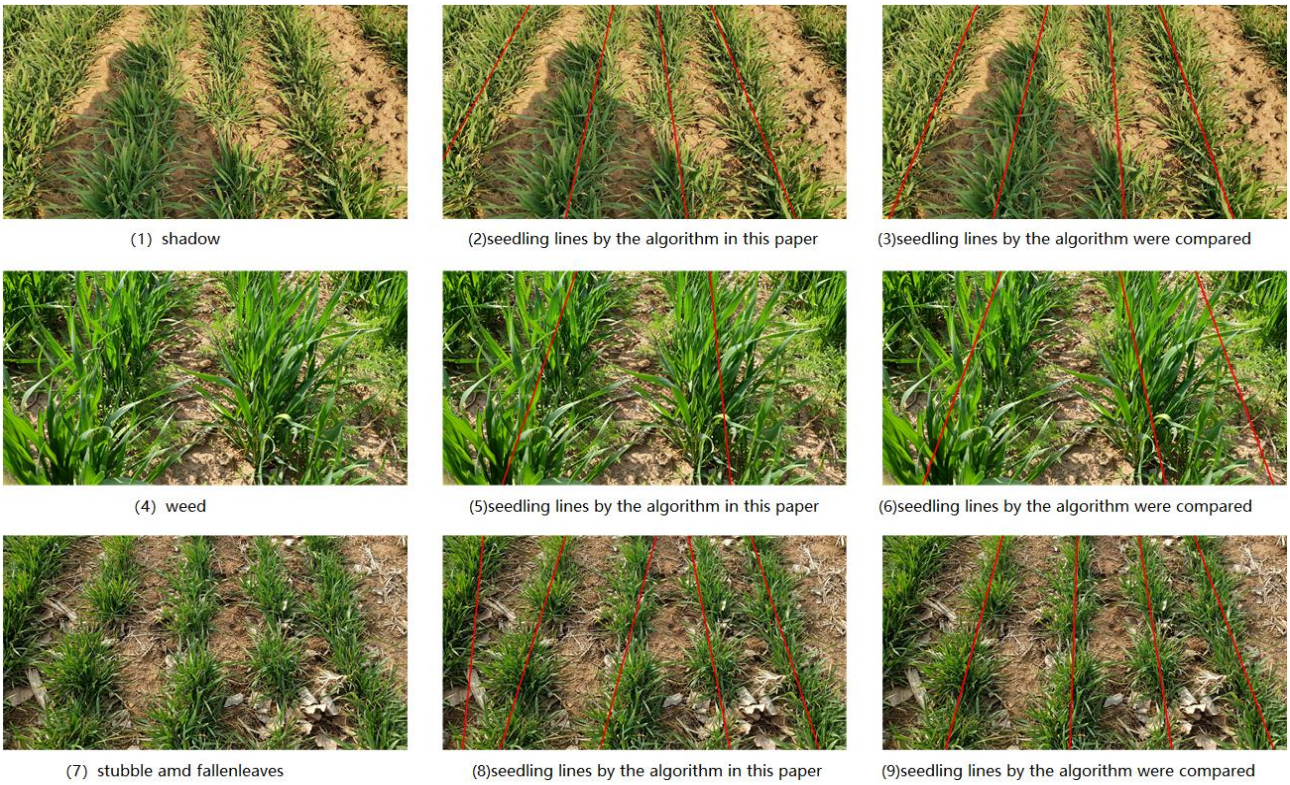

Fig. 12 - The wheat seedling lines under shadows, weeds, stubble and leaves obtained by two algorithms

To compare the performance of the two algorithms under different environmental backgrounds, 30 wheat seedling images each were selected from the dataset that had varying conditions such as strong light, low light, shadows, weeds, stubble, and fallen leaves. As can be seen from Figure10, light has little influence on the extraction effect of the proposed algorithm, but has some influence on the previous algorithm. As shown in Figure 10(3), strong light will increase the vertical projection value. Once the value exceeds the preset threshold, it is considered that there may be wheat seedling rows in the area. Therefore, when the light is strong, the previous algorithm will extract the wheat seedling line excessively, and when the light is dark, it will miss to extract the wheat seedling line.

Figure 11 shows the extraction effects of the two algorithms under the background of shadows, weeds, stubble and fallen leaves. As can be seen from the figure, the algorithm in this paper is less affected by shadow and weed environment, while more affected by stubble and fallen leaves. Through analysis, it is found that more corner points are detected in the stubble and fallen leaves area in the figure. Due to their irregular distribution in the image, sometimes the error of the extracted wheat seedling line is large. As for the previous algorithm, it is little affected by shadow, stubble and fallen leaves, but it is affected by weeds, and it is easy to misidentify the weeds between the rows as wheat seedlings.

Table 3

The evaluation statistics of wheat seedling lines in different background environment under two algorithms

Algorithm	Categories	Range error / pixel	Angle error / °
Textual algorithm	Intense light	9.06	0.87
	Dim light	10.69	0.95
	Shadow	11.54	0.94
	Weed	14.75	1.23
	Stubble and fallen leaves	19.58	1.69
Previous algorithm	Intense light	23.77	1.96
	Dim light	20.23	1.85
	Shadow	18.51	1.72
	Weed	28.94	2.90
	Stubble and fallen leaves	18.84	1.66

Table 3 shows the evaluation statistics of the two algorithms under different environmental backgrounds. As can be seen from the table, the extraction effect of the proposed algorithm is still better than the previous algorithm in terms of error. But the extraction accuracy is relatively low in the background of weeds, stubble and fallen leaves. In addition, the extraction accuracy of the previous algorithm is worse in the background of weeds.

Comparison of wheat seedling line extraction under different yaw angles

During real-world agricultural machinery operations in the fields, the uneven ground, mechanical vibration and crop line bending and other problems will inevitably lead to a certain yaw angle of the camera for image acquisition. Therefore, a robust crop row extraction method should be equally applicable to images captured with a non-zero yaw angle. In order to study the influence of yaw angle on the algorithm in this paper, 30 images with small yaw angle and 30 images with large yaw angle were selected from the wheat seedling data set respectively. In this paper, small yaw angle refers to less than 30°, and large yaw angle refers to greater than 30°. As shown in Figure 13, it can be seen that the wheat seedling line extracted by the algorithm in this paper has a higher accuracy, while the previous algorithm has a lower accuracy.

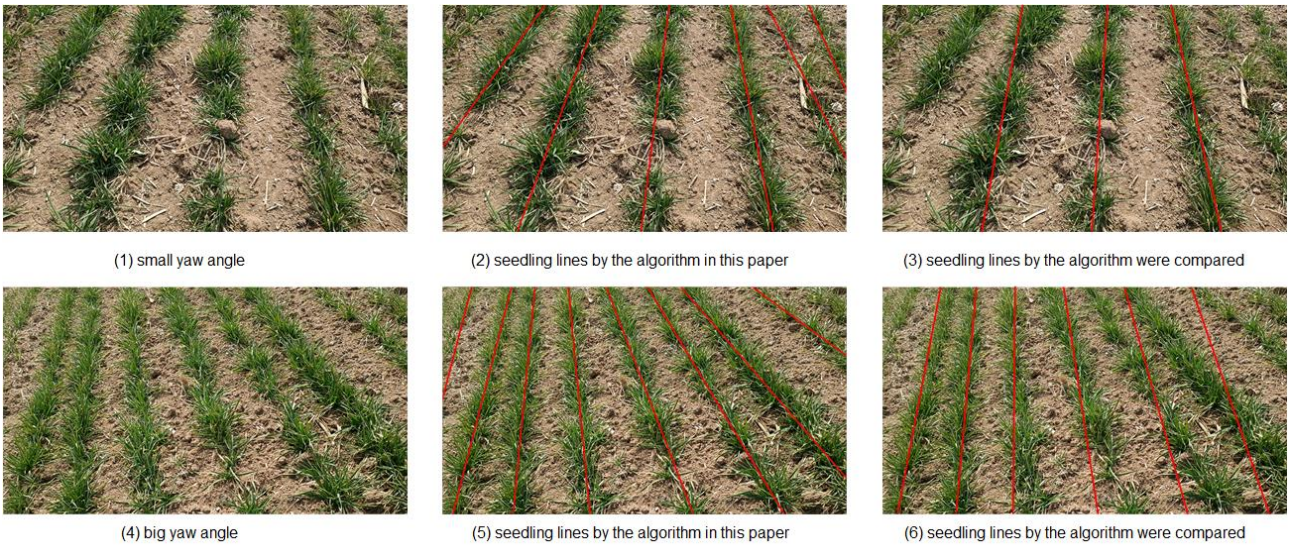

Fig. 13 - The wheat seedling lines at different yaw angles obtained by two algorithms

Table 4 shows the statistics of evaluation results of the two algorithms under different yaw angles. As can be seen from the table, the algorithm in this paper is less affected by yaw angle, while the previous algorithm is more affected by yaw angle, especially when the yaw angle is larger, its angle error can reach 8.46°.

Table 4

The evaluation statistics of wheat seedling lines at different yaw angles under two algorithms

Algorithm	Categories	Range error / pixel	Angle error / °
Textual algorithm	Small yaw angle	10.27	0.97
	Big yaw angle	13.54	1.18
Previous algorithm	Small yaw angle	42.61	3.89
	Big yaw angle	77.84	8.46

Based on the analysis of the above aspects, the wheat seedling line obtained by the algorithm in this paper is less than the previous algorithm in terms of distance error and angle error, and it has strong robustness under various environmental conditions.

Comparative analysis of real-time performance of the algorithm

In the above test process, the running time of the two algorithms for each image was recorded, and the average running time under each specific classification was calculated, as shown in Table 5. From the table, it can be observed that for wheat seedling images of size 1920×1080 pixels, the average runtime of the proposed algorithm for extracting wheat row lines ranges from 67 ms to 71 ms, while the previous algorithm's average runtime for the same task ranged from 50 ms to 55 ms. Therefore, the textual algorithm is 12 ms-21 ms slower than the previous algorithm. However, this time difference has no great impact on the field experiment, and it can still meet the real-time requirements of the job.

Table 5

Running time statistics of two algorithms

Items	Specific classification	Textual algorithm	Previous algorithm
Different years	2019	67.44 ms	52.23 ms
	2020	68.73 ms	51.65 ms
	2021	69.68 ms	52.94 ms
	2022	67.82 ms	53.61 ms
Different period of rejuvenating	Initial stage	68.99 ms	51.29 ms
	Middle stage	69.42 ms	52.47 ms
	Later stage	68.37 ms	52.67 ms
Different environmental background	Intense light	68.81 ms	52.19 ms
	Dim light	69.03 ms	51.42 ms
	Shadow	68.61 ms	51.00 ms
	Weed	68.33 ms	50.76 ms
	Stubble and fallen leaves	70.11 ms	52.98 ms
Different yaw angles	Small yaw angle	67.25 ms	53.44 ms
	Big yaw angle	68.43 ms	54.76 ms

CONCLUSIONS

This paper addresses the extraction of navigation lines for wheat root cutting and proposes a deep learning algorithm based on an improved YOLOv5 model. The algorithm's performance is tested and analyzed through field experiments, leading to the following key conclusions: (1) The measurement of the position error of the navigation line at different speeds shows that the average and standard deviations of the actual position error of the navigation path increase with the speed. The navigation effect is the best when the system operates at 1 m/s, and the maximum, average and standard deviation of the position error are 58 mm, 18.56 mm and 3.96 mm, respectively. (2) The improved algorithm and the original algorithm were tested by using the collected data from 2019-2022, and compared from four aspects: different years, different periods of rejuvenation, different environments and different yaw angles. The improved algorithm is superior to the original algorithm and has strong robustness under various circumstances.

ACKNOWLEDGEMENT

The research of this paper is funded by Natural Science Foundation of Shandong Province (ZR2021MF096). During the project, the help of Qingdao Zongsen Agricultural Machinery Research Institute and Qingbao Agricultural Machinery Station is greatly appreciated.

REFERENCES

[1] Amrani, A., Sohel, F., Diepeveen, D., Murray, D., Jones, M. G. K. (2023) Deep learning-based detection of aphid colonies on plants from a reconstructed Brassica image dataset. *Computers and Electronics in Agriculture,* Vol. 205. February 2023, 107587. England.

[2] Dhruba, N., Abhishek, S., Kshetrimayum, T. C. (2018). Multipurpose GPS Guided Autonomous Mobile Robot. *Progress in Advanced Computing and Intelligent Engineering*, Vol.564, pp. 361-372. Springer Singapore.

[3] He, J., Zhang, Y., Luo, X., Zhao, R., He, J. et al (2021). Visual detection of rice rows based on Bayesian decision theory and robust regression least squares method. *International Journal of Agricultural and Biological Engineering,* Vol. 14(1), pp. 199-206. China.

[4] Huo, W. G., Lv, Z. Q., Shao, J. (2004). Design of multi-functional root cutting machine for winter wheat (手扶式冬小麦多功能断根机设计). *Shandong Agricultural Machinery,* 2004(06), pp.11-13. *Shandong/China.*

[5] Jeon, C.-W., Kim, H.-J., Yun, C., Gang, M., Han, X. (2021). An entry-exit path planner for an autonomous tractor in a paddy field. *Computers and Electronics in Agriculture,* Vol.191, December 2021, 106548. England.

[6] Jiang, G. Q., Wang, X. J., Wang, Z. H., Liu, H. M. (2016). Wheat rows detection at the early growth stage based on Hough transform and vanishing point. *Computers and Electronics in Agriculture*, Vol. 123, pp. 211-223. England.

[7] Jiang, Y., Zhang L. L., Xue, P., Wang X. D. (2021). Development Status of Wheat Industry in China and International Experience for Reference (我国小麦产业发展情况及国际经验借鉴). *Journal of Agricultural Science and Technology*, Vol. 23(07), pp. 1-10. Beijing/China.

[8] Khan, S., Tufail, M., Khan, M. T., Khan Z. A., & Anwar, S. (2021). Deep learning-based identification system of weeds and crops in strawberry and pea fields for a precision agriculture sprayer. *Precision Agriculture,* Vol. 22(6), pp. 1-17. Netherlands.

[9] Li, C. Z., Zhu, G. Y., (2006). Design and research of a new type of winter wheat root cutting machine (一种新型冬小麦断根机的设计研究). *Farm Machinery*, Vol. 2006(22), pp. 80-81. *Beijing/China.*

[10] Li, X. G., Zhao, W., Zhao, L. L. (2021). Extraction algorithm of the center line of maize row in case of plants lacking. *Transactions of the Chinese Society of Agricultural Engineering (Transactions of the CSAE)*, Vol. 37(18), pp. 203-210. Beijing/China.

[11] Liu, F.C., Yang, Y., Zeng, Y.M., Liu Z. Y. (2020). Bending diagnosis of rice seedling lines and guidance line extraction of automatic weeding equipment in paddy field. *Mechanical Systems and Signal Processing,* Vol. 142(C), pp. 106791-106791. England.

[12] Liu, G., Nouaze, J. C., Mbouembe, P. L. T., Kim, J. H. (2020). YOLO-tomato: A robust algorithm for tomato detection based on YOLOv3. *Sensors,* Vol. 20(7), pp. 2145-2145. Switzerland.

[13] Lv, Z. Q., Li, R. Z., Dong, Q. Y., Yin, K. R., Yu, S. L. (2006). Mechanical root-cutting models for increasing the yield of winter wheat (冬小麦增产技术中机械断根方式的研究). Transactions of the Chinese Society of Agricultural Engineering, Vol. 2006(04), pp. 103-106. Beijing/China.

[14] Pang, Y., Shi, Y., Gao, S. C., Jiang, F., Veeranampalayam-Sivakumar, A., Thompson, L., Luck, J., Liu, C. (2020). Improved crop row detection with deep neural network for early-season maize stand count in UAV imagery. *Computers and Electronics in Agriculture,* Vol. 178, pp. 105766. England.

[15] Sevilla, M. F. de, Gutiérrez, Ó., Gómez, J., Tayebi, A., Álvarez, Á., Adana, F. S. de. (2021). On the application of radio planning tools in open environments for the improvement of autoguidance systems used in precision agriculture. *Computers and Electronics in Agriculture*, Vol. 187, August 2021, 106258. England.

[16] Villacrés, J., Viscaino, M., Delpiano, J., Vougioukas, S., Cheein, F. A. (2023). Apple orchard production estimation using deep learning strategies: A comparison of tracking-by-detection algorithms. *Computers and Electronics in Agriculture,* Vol. 204, January 2023, 107513. England.

[17] Yadav, P. K., Thomasson, J. A., Hardin, R., Searcy, S. W., Braga-Neto, U., Popescu, S. C., Martin, D. E., Rodriguez, R., Meza, K., Enciso, J., Diaz, J. S., Wang, T. (2023) Detecting volunteer cotton plants in a corn field with deep learning on UAV remote-sensing imagery. *Computers and Electronics in Agriculture*, Vol. 204, January 2023, 107551. England.

[18] Yang, X., Yan. J. (2020). Arbitrary-Oriented Object Detection with Circular Smooth Label. *European Conference on Computer Vision.* 2020, pp. 677-694. Springer: Cham.

[19] Yang, X., Yang, J., Yan, J., Zhang, Y., Zhang, T., Guo, Z., Xian, S., Fu, K. (2019). Scrdet: towards more robust detection for small, cluttered and rotated objects. *2019 IEEE/CVF International Conference on Computer Vision. South Korea: IEEE*, 2019, pp. 8232-8241. South Korea.

[20] Yu, S. L., Qi, X. H., Liu, X. Y., Dong Q. Y., Xu, Y. M. (1985). Studies on The Effect on Yield Increase by Deep Cultivation Root Cutting in Winter Wheat (冬小麦深耘断根增产作用的研究). *Scientia Agricultura Sinica*, Vol. 1985(04), pp. 30-35. Beijing/China.

[21] Yun, C., Kim, H.-J., Jeon, C.-W., Gang, M., Lee, W. S., Han, J. G. (2021). Stereovision-based ridge-furrow detection and tracking for auto-guided cultivator. *Computers and Electronics in Agriculture*, Vol. 191, December 2021, 106490. England.